Am J Cancer Res 2023;13(4):1407-1424
www.ajcr.us /ISSN:2156-6976/ajcr0143362

Original Article

Improving the anti-tumor effect of EGCG in colorectal cancer cells by blocking EGCG-induced YAP activation

Yu Wang[1*], Sha-Sha Jin[1*], Dan-Ting Li[1*], Xiao-Chun Jiang[1,3], Afrasiyab[1], Anam Khalid[1], Xin Liu[1], Hui-Lin Wang[1], Hai-Yan Wang[1], Zai-Gui Wang[1], Zhong-Wen Xie[2], Shou-Jun Huang[1,3]

[1]School of Life Sciences, Anhui Agricultural University, Hefei 230036, Anhui, China; [2]State Key Laboratory of Tea Plant Biology and Utilization, Anhui Agricultural University, Hefei 230036, Anhui, China; [3]Anhui International Joint Research and Developmental Center of Sericulture Resources Utilization, Hefei 230036, Anhui, China. [*]Equal contributors.

Received April 6, 2022; Accepted March 19, 2023; Epub April 15, 2023; Published April 30, 2023

Abstract: (-)-Epigallocatechin-3-gallate (EGCG) is the primary active ingredient in green tea and has been used for cancer prevention in clinical trials. The anti-tumor effects of EGCG stem from its ability to inhibit the activities of many oncoproteins, such as AKT, VEGFR, STAT3, and mutant p53. However, the clinical efficacy of EGCG is unsatisfactory. How to improve the anti-tumor effects of EGCG is an open question. Here we report that EGCG inhibits the tumor suppressive Hippo signaling pathway and activates downstream YAP in colorectal cancer (CRC) cells. Activation of YAP impedes the anti-tumor effects of EGCG. YAP blockade increases the sensitivity of CRC cells to EGCG treatment.

Keywords: EGCG, Hippo, LATS1/2, YAP

Introduction

Colorectal cancer (CRC), one of the most commonly diagnosed malignancies in both sexes, is the second leading cause of cancer related death worldwide. CRC had a global incidence rate of 6.1% and a mortality rate of 9.2% in 2018 [1]. Moreover, the incidence and mortality rates of CRC are rapidly increasing worldwide, and the public health burden of CRC is expected to increase by 60% in 2030 [2]. CRC can be classified as sporadic, familial, or inflammation-dependent CRC, among these three types, sporadic CRC accounts for approximately 75% of cases [3-5]. Current CRC therapeutic approaches include surgery, chemotherapy, and radiotherapy. Metastatic tumors are usually not amenable to surgical resection. Due to primary or acquired multidrug resistance (MDR), CRC patients either respond poorly to chemotherapy or have a high risk of tumor relapse [6, 7]. Thus, it is important to understand the molecular mechanisms of MDR in CRC and develop novel strategies to improve anti-tumor effect.

The Hippo signaling pathway was named after Hpo, a *Drosophila* serine/threonine kinase identified by several groups in 2003. The Hippo pathway has emerged as a highly conserved tumor suppressor pathway that controls organ size and tissue homeostasis [8]. The core Hippo pathway consists of a kinase cascade: the upstream sterile 20-like protein kinases (STK3/MST2 and STK4/MST1) form complexes with their adapter protein, Salvador family WW domain containing protein 1 (WW45). The MST1/2-WW45 complex phosphorylates and activates a downstream kinase complex consisting of large tumor suppressor kinase 1/2 (LATS1/2) and its adapter proteins, MOB kinase activator 1A (MOB1A) and MOB1B [9]. Yes-associated protein (YAP) and transcriptional coactivator with PDZ-binding motif (TAZ) are the major downstream transcription coactivators of the Hippo pathway [10, 11]. The phosphorylation of YAP/TAZ at consensus HXRXXS motifs by LATS1/2 promotes the cytoplasmic retention of YAP/TAZ by 14-3-3 proteins, and reduces cytoplasmic YAP/TAZ levels by facilitating their ubiquitination and proteasomal degradation by the

E3 ligase SCF (β-TrCP) [10-13]. When Hippo signaling activity is compromised, dephosphorylated YAP/TAZ accumulates and is translocated into the cell nucleus where it interacts with TEA domain transcription factors 1-4 (TEAD1-4) and activates the transcription of multiple target genes [14]. The Hippo signaling pathway is frequently inactivated in multiple human cancer types, including CRC [15, 16]. Furthermore, YAP activation and elevated expression of YAP target genes play important roles in CRC tumorigenesis, progression, and metastasis [17].

Green tea, produced from the leaves of the Camellia sinensis plant, is one of the most popular beverages worldwide [18]. The components of green tea are well characterized and have been studied for their beneficial effects on human health, including antioxidant effects, antibacterial activities, neuroprotective roles, cardioprotective effects, and anticancer effects [19, 20]. These health benefits are generally attributed to green tea polyphenols, particularly catechins. The four most abundant catechins in green tea are epicatechin (EC), epicatechin-3-gallate (ECG), epigallocatechin (EGC), and epigallocatechin-3-gallate (EGCG) [21]. EGCG accounts for approximately 50% of green tea polyphenols and its function in cancer prevention, such as in gastric cancer, breast cancer, and CRC, has been extensively investigated *in vitro*, *in vivo* and over epidemiological studies in the last few decades [22-25]. For example, Stalmach et al. (2010) reported that after consumption of green tea, approximately 70% of EGCG reaches the colon where it may effectively interact with colorectal epithelial or CRC cells [26]. In recent years, the antineoplastic mechanisms of EGCG in CRC have been well characterized and include activation of the NF-κB signaling pathway, activation of 67LR dependent cell apoptosis, inhibition of bFGF expression, and inhibition of GSK3alpha and beta activity, among others [27-30].

In this study, we discovered that EGCG can inhibit Hippo signaling activity and activate the proliferative and anti-apoptotic roles of YAP in CRC cells *in vitro*, thus resulting in insensitivity to EGCG treatment. Mechanistically, EGCG promotes the ubiquitination and proteasomal degradation of Hippo signaling core kinases LATS1/2 by the E3 ubiquitin ligase C-terminus of Hsc70-interacting protein (CHIP). In turn, LATS1/2 degradation leads to YAP hypo-phosphorylation, accumulation and translocation into the cell nucleus, where it upregulates the transcription of YAP target genes and antagonizes EGCG treatment. Inhibition of YAP-TEADs interaction and knockdown of YAP sensitized CRC cells to EGCG-induced cytotoxicity. We conclude that the combination of YAP inhibition and EGCG treatment showed synergistic antitumor effects in CRC cells.

Materials and methods

Reagents and antibodies

EGCG was obtained from Sigma-Aldrich (St. Louis, MO, USA) and dissolved in water. Lipofectamine 3000 was purchased from Invitrogen (Carlsbad, CA, USA). Anti-GAPDH antibody was purchased from Proteintech (Hubei, China). Anti-alpha-Tubulin antibody was purchased from ABclonal Technology (Beijing, China). Anti-LATS1, anti-LATS2, anti-phospho-LATS1/2 Thr-1079, anti-phospho-LATS1 Ser909, anti-YAP, anti-phospho-YAP Ser127, anti-phospho-YAP Ser381, anti-TAZ, anti-Lamin A/C, anti-MOB1, anti-phospho-MOB1 Thr35, anti-MST1/2, and anti-WW45 antibodies were purchased from Cell Signaling Technology (Danvers, MA, USA). Anti-Flag, anti-Myc and anti-HA antibodies were purchased from Medical & Biological Laboratories (MBL, Japan). Anti-heat shock protein 70 (HSP70), anti-CHIP, and anti-ubiquitin antibodies were purchased from Abcam (Waltham, MA, USA).

Plasmids

For LATS1 and YAP expression, the human LATS1 and YAP coding sequences (CDS) were PCR-amplified from total HEK293T cDNA with TransStart FastPfu DNA Polymerase (Transgen, Beijing, China) and ligated into the pEF-3xFlag vector. The complete human CHIP CDS was PCR amplified from total HEK293T cDNA, full-length CHIP and two CHIP deletion mutants comprising 1) amino acids 1-189 (CHIP delta TPR) and 2) 135-303 (CHIP delta U-box) were inserted into pEF-Myc vector. HA-LATS2 was a gift from Professor Jae Hong Seol's lab (Seoul National University, Korea), and used as a PCR template for pEF-Flag-LATS2 cloning. We introduced K30A, H260Q, I235A, and R272A, in CHIP to generate CHIP loss-of-function mutants using the Fast Mutagenesis System (Transgen).

We also generated pEF-Flag-YAP S127A and pEF-Flag-YAP S381A mutations with the same method. pEF-Flag-YAP 5S/5A (S61/109/127/164/381A) mutations were introduced using the Fast Multisite Mutagenesis System (Transgen). ShRNA sequence for CHIP or YAP knockdown were chosen from verified literature and cloned into the AgeI/EcoRI sites of the pLKO.1 vector.

pLKO.1-shCHIP-1: CCGGGAAGAGGAAGAAGCGAGACATCTCGAGATGTCTCGCTTCTTCCTCTTCTTTTTG; pLKO.1-shCHIP-2: CCGGGCAGTCTGTGAAGGCGCACTTCTCGAGAAGTGCGCCTTCACAGACTGCTTTTT; pLKO.1-shYAP-1: CCGGGCCACCAAGCTAGATAAAGAACTCGAGTTCTTTATCTAGCTTGGTGGCTTTTTG; pLKO.1-shYAP-2: CCGGCAGGTGATACTATCAACCAAACTCGAGTTTGGTTGATAGTATCACCTGTTTTTG.

All constructs were verified by Sanger sequencing.

Cell lines, cell culture, transfection, and infection

HEK293T cells were cultured in Dulbecco's modified Eagle's medium (DMEM) (Gibco, USA) supplemented with 10% fetal bovine serum (FBS). Human HCT116 CRC cell line was gifted from Dr. Dahua Chen's laboratory in 2016. SW620 cell line was purchased from the National Collection of Authenticated Cell Cultures (Shanghai, China) in 2019. RKO and LoVo cells were purchased from the American Type Culture Collection (Rockville, MD, USA). The provider performed cell line authentications via DNA fingerprinting. Determination of cell vitality and assessment of mycoplasma contamination were performed with PCR based assay in our lab. HCT116 cells were cultured in RPMI-1640 medium (Gibco BRL, NY, USA) supplemented with 10% heat-inactivated FBS (Hyclone, Yokohama, Japan). RKO and SW620 cells were grown in DMEM containing 10% FBS. All cell lines were maintained in the logarithmic phase of growth at 37°C in a humidified incubator with 5% CO_2 in air. Cells used in experiments were within 10 passages of thawing. Trypsin, phosphate-buffered saline (PBS), penicillin, streptomycin and glutamine (100X) were obtained from Gibco.

Cells were transfected with overexpression constructs using Lipofectamine 3000 (Invitrogen, CA USA) according to the manufacturer's protocol. In transient transfection experiments, plasmid DNA was kept constant with the empty vector. shRNAs were delivered via infection with lentiviruses produced by co-transfection of HEK293T cells with pLKO.1-shScramble, pLKO.1-shCHIP, or pLKO.1-shYAP plasmids and packaging plasmids (psPAX2 and pMD2.G). Stable pools were selected with 2 μg/mL of puromycin (Amresco, TX, USA) for 5 days.

RNA preparation, reverse transcription, and quantitative real-time PCR (qPCR)

RNA was isolated using TRIzol reagent according to the manufacturer's instructions (Invitrogen). Next, 1 μg of RNA was mixed with Oligo(dT) and random primers and reverse transcribed into complementary DNA (cDNA) using the PrimeScript™ II 1st Strand cDNA Synthesis Kit (TaKaRa, Japan). Subsequently, diluted cDNA was used for qPCR analysis using TransStart Top Green qPCR SuperMix (Transgen) on an LC480 II Real-Time PCR System (Roche, Switzerland). In all experiments, GAPDH RNA served as the internal (normalization) control and calibrator controls were chosen appropriately. Human PCR primers were as follows: LATS1, sense-5'-AAACCAGGGAATGTGCAGCAA-3', antisense-5'-CATGCCTCTGAGGAACTAAGGA-3'; LATS2, sense-5'-ACCCCAAAGTTCGGACCTTAT-3', antisense-5'-CATTTGCCGGTTCACTTCTGC-3'; YAP, sense-5'-CCTCGTTTTGCCATGAACCAG-3', antisense-5'-GTTCTTGCTGTTTCAGCCGCAG-3'; CTGF, sense-5'-GTGGAGTATGTACCGACGGC-3', antisense-5'-GCAGGCACAGGTCTTGATGA-3'; CYR61, sense-5'-CTGCGAAGATGGGGAGACAT-3', antisense-5'-GCCTGTAGAAGGGAAACGCT-3'; ANKRD1, sense-5'-GGAGATACCCCGTTGCATGA-3', antisense-5'-TGTTGAGATCCGCGCCATAC-3'; ABCC1, sense-5'-CTCTATCTCTCCCGACATGACC-3', antisense-5'-AGCAGACGATCCACAGCAAAA-3'; ABCB1, sense-5'-AGGAGGCCAACATACATGCC-3', antisense-5'-GCTGTCTAACAAGGGCACGA-3'; ABCG2, sense-5'-CAGGTGGAGGCAAATCTTCGT-3', antisense-5'-ACCCTGTTAATCCGTTCGTTTT-3'; E-Cadherin, sense-5'-CAGCCACAGACGCGGACGAT-3', antisense-5'-CTCTCGGTCCAGCCCAGTGGT-3'; ZO-3, sense-5'-GTGGGGGCCGATTGACTGTT-3', antisense-5'-GTGTGCTGTTCCCAGATGGTC-3'; N-Cadherin, sense-5'-TTGAGCCTGAAGCCAACCTT-3', antisense-5'-TGTAGGTGGCCACTGTGCTTAC-3';

Vimentin, sense-5'-TGGCCGACGCCATCAACAC-C-3', antisense-5'-TGCTGCTCCAGGAAGCGCA-C-3'; Snail, sense-5'-GCACATCCGAAGCCAC-AC-3', antisense-5'-GGAGAAGGTCCGAGCACA-3'; Slug, sense-5'-TTCGGACCCACACATTACCT-3', antisense-5'-TTGGAGCAGTTTTTGCACTG-3'; GAPDH, sense-5'-CTGGGCTACACTGAGCACC-3', antisense-5'-AAGTGGTCGTTGAGGGCAATG-3'. The relative expression levels of the target genes were calculated as $2^{-[(\Delta Cp \text{ of gene}) - (\Delta Cp \text{ of GAPDH})]}$, where Cp represents the threshold cycle for each transcript.

Immunoblotting

Cells were treated as indicated in the figures, and washed twice with ice-cold PBS. Then cells were harvested in a lysis buffer (50 mM Tris (pH 7.4), 150 mM NaCl, 1 mM ethylenediaminetetraacetic acid (EDTA), 1 mM ethylene glycol tetraacetic acid (EGTA), 1% Triton X-100, 0.5 mM dithiothreitol (DTT), 2.5 mM sodium pyrophosphate ($Na_4P_2O_7$), 50 mM sodium fluoride (NaF), 1 mM sodium vanadate (Na_3VO_4) and 2 mM phenylmethylsulfonyl fluoride (PMSF)) with protease inhibitor cocktail (APExBIO, TX, USA) for 30 min. Lysates were centrifuged at 13,000 rpm for 15 min at 4°C. The total protein concentrations were determined using Bradford reagent. The supernatants were mixed with equal volumes of Laemmli sample buffer and boiled for 10 min, and 25 μg of each protein sample was subjected to SDS-PAGE using 8% or 10% gels. The proteins were electrophoretically transferred to nitrocellulose membrane and probed for 3 hr at room temperature or overnight at 4°C with the indicated antibodies. After several washing steps, the membranes were incubated for 60 min with horseradish peroxidase-conjugated secondary antibodies (Biosharp, Beijing, China) and washed seven times for 5 min each. The proteins of interest were visualized with Super Signal West Pico chemiluminescent substrate (Pierce Biotechnology, Rockford, IL, USA). Chemiluminescent imaging was performed with a Tanon-5200 Chemiluminescent Imaging System (Tanon Science & Technology, Shanghai, China). Densitometric scanning of immunoblots was performed using ImageJ software (Bethesda, MD, USA).

Co-immunoprecipitation

Cells were lysed in immunoprecipitation buffer (50 mM Tris-HCl pH 7.4, 150 mM NaCl, 1% Nonidet P-40, 10% glycerol, 50 mM NaF, 1 mM Na_3VO_4, 2 mM PMSF and 1 mM EDTA) containing protease inhibitors on ice for 30 min and then clarified by centrifugation at 15,000×g for 15 min at 4°C. A fraction of each cleared lysate was reserved as inputs, and the remainder was precleared with a 50% suspension of protein A/G-Sepharose beads (Amersham Biosciences, WI, USA). Each sample was immunoprecipitated for 2 hr at 4°C with 5 μg of the appropriate antibodies on protein A/G-Sepharose beads or Flag-Beads (Sigma Aldrich). Immunocomplexes were washed four times with lysis buffer and eluted by boiling in Laemmli sample buffer. The precipitates were examined via western blotting using the indicated antibodies.

In vivo ubiquitination assay

For ubiquitination assays, HCT116 cells in 6-cm dishes were transfected with the indicated plasmids for 48 hr. 6 hr prior to cell harvesting, 20 μM of MG132 (Calbiochem, Germany) was used to inhibit proteasome activity. For immunoprecipitation, centrifuged cell pellets were boiled in 300 μL of SDS lysis buffer (50 mM Tris-HCl, pH 6.8, 1.5% SDS) for 15 min. Then, 250 μL of boiled protein lysates were diluted with 3 ml ice-cold EBC/bovine serum albumin (BSA) buffer (50 mM Tris-HCl, pH 6.8, 180 mM NaCl, 0.5% CA630, 0.5% BSA) containing protease inhibitors. Lysates were incubated with the indicated antibodies overnight and then conjugated to protein A/G beads (Amersham Biosciences) for 2 hr at room temperature. The beads were collected by centrifugation at 5,000xg for 3 min at 4°C and washed 5 times with ice-cold EBC/BSA buffer. Immunocomplexes were resuspended and boiled with 30 μL of Laemmli sample buffer and subjected to Immunoblotting. Polyubiquitylated proteins were detected with anti-ubiquitin antibodies.

Cytosol/nuclear protein fractionation

For cytosol/nuclear protein fractionation, HCT-116 cells treated as indicated in the figures were pelleted and resuspended in 3 relative volumes of hypotonic buffer (20 mM HEPES pH 7.4, 5 mM NaF, 1 mM Na_3VO_4, 1 mM EDTA) supplemented with Protease Inhibitor Cocktail (APExBIO) and 1 mM DTT. Upon incubation on ice for 20 min, 0.5% Triton X-100 was added and mixed well, and lysates were centrifuged at 13,000 rpm for 30 s at 4°C to collect the cyto-

solic fractions. The nuclear pellets were then resuspended in 1 volume of nuclear lysis buffer (20 mM HEPES, pH 7.4, 25% glycerol, 420 mM NaCl, 1.5 mM $MgCl_2$, 1 mM EDTA) supplemented with Protease Inhibitor Cocktail and 1 mM DTT. Nuclei were incubated for 30 min at 4°C with constant agitation and then centrifuged at 13,000 rpm for 30 min at 4°C. To decrease the salt concentration of the nuclear fractions, sample were adjusted with 1 volume of nuclear lysis buffer without NaCl, supplemented with Protease Inhibitor Cocktail and 1 mM DTT. Cytosolic and nuclear fractions were analyzed by Immunoblotting. alpha-Tubulin and Lamin A/C served as controls for the cytosolic and nuclear fractions, respectively.

Immunofluorescence staining

HCT116 cells were seeded on sterile glass coverslips in 6-well plates and treated with EGCG for the indicated times. All samples were fixed for 20 min with 4% formaldehyde in PBS and incubated in 0.5% Triton X-100 for 20 min at room temperature. After three washings with PBS, all slides were incubated 1 hr with blocking buffer (5% BSA in PBS) and then stained with primary antibody against YAP overnight at 4°C. After five washings with PBS, all slides were incubated with fluorescent-labeled secondary antibody and DAPI (Sigma) in the dark at room temperature. Slides were analyzed by confocal microscopy (Zeiss, LSM 880, Germany).

Dual-luciferase reporter assay

For luciferase assays, 2×10^4 HCT116 cells were seeded in 96-well plates, grown to 70% confluence and co-transfected with the 8xGTIIC-luciferase reporter, Renilla and the indicated plasmids. 36 hr after transfection, cells were treated for the indicated times and lysed. Luciferase activity was detected with the SpectraMax i3 luminometer (Molecular Devices, CA, USA) and the dual luciferase assay system (Promega, WI, USA) following the manufacturer's instructions. Firefly-luciferase activity was normalized to Renilla-luciferase activity to evaluate activity. Each group was assessed in triplicate.

Chromatin immunoprecipitation (ChIP) assay

For ChIP experiments, 150 mm dishes of Flag-YAP overexpressing HCT116 cells were treated with EGCG for the indicated times. Samples were then fixed with 1% formaldehyde at room temperature for 10 min to crosslink chromatin proteins with genomic DNA and neutralized with a final concentration of 0.125 M freshly prepared glycine for 5 min. Cells were lysed in lysis buffer (50 mM Tris-HCl pH 8.1, 10 mM EDTA, 1% SDS and protease inhibitors) and the resulting lysates were sonicated to shear chromatin into fragments with an average length of ~300-500 bp. Lysates were precleared with a 50% suspension of protein A/G-Sepharose beads (Amersham Biosciences) and immunoprecipitated with 40 µL of Flag-beads (Sigma Aldrich). The immunoprecipitated DNA fragments were then purified. PCR was then performed with specific primers to determine whether EGCG affects the binding of YAP to *CTGF* and *CYR61*. The ChIP primers were as follows: CTGF, sense-5'-CGCCAATGAGCTGAATGGAGT-3', antisense-5'-TGAGTGTCAAGGGGTCAGGAT-3'; CYR61, sense-5'-AAAGGTGCAATGGAGCCAGG-3', antisense-5'-GTGTTGCAGTGACGTCGG-3'.

MTT (3-(4,5-dimethylthiazol-2-yl)-2,5-diphenyltetrazolium bromide) assay

For MTT assays, cells were seeded at a concentration of 5×10^3 cells/mL into 96-well plates and grown overnight. Then the cells were transferred into serum-free DMEM for another 12 hr. After serum starvation, the cells were treated with EGCG at the indicated concentrations and for the indicated number of days. Cell proliferation was evaluated with the MTT assay. Briefly, 10 µL of MTT solution (5 mg/mL, Roche, Switzerland) was added to each well and incubated for 4 hr at 37°C. Then the supernatant was aspirated and the MTT-formazan crystals formed by metabolically viable cells were dissolved in 150 µL of DMSO. Finally, the absorbance was monitored with a microplate reader at a wavelength of 490 nm.

Flow cytometric analysis of the cell cycle and apoptosis

Cells were treated with various concentrations of EGCG for the designated times. The cells were then harvested and processed according to the manufacturer's protocols, as follow. For cell cycle analysis, propidium iodide (PI) from Biosharp was used. Cells were then analyzed on a BD FACSCalibur flow cytometer (BD, NJ,

USA). Data analysis was performed with FlowJo software (San Carlos, CA, USA). The FITC Annexin V and PI apoptosis assays were performed with the Annexin V-FITC/PI Apoptosis detection Kit (Meilunbio, Liaoning, China). Briefly, 1×10^6 cells were collected by centrifugation, resuspended in binding buffer, stained with fluorochrome-conjugated Annexin V and PI, and quantified with a BD FACSCalibur flow cytometer.

EdU labeling assay

EdU labeling assays were performed in 24-well plates using the EdU Cell Proliferation Assay Kit (APExBIO). After EGCG treatment, EdU was added to each well, and incubated for 3 hr at 37°C. EdU-positive cells from 10 fields (200× magnification) were examined and counted. Results were presented as the mean number ± SD of EdU-positive cells across independent experiments.

Detection of intracellular reactive oxygen species (ROS) generation

Intracellular ROS were detected by immunofluorescence. Cells were seeded in a 24-well cell culture plate and incubated for 24 hr. Then, the cells were treated with EGCG for 24 hr. Medium with DMSO was used as the control group. Following treatment, cells were stained with 5 μM of DCFH-DA (Solarbio, Beijing, China) at 37°C for 30 min in the dark. Finally, cells were incubated in serum-free DMEM and ROS expression was observed using an inverted fluorescence microscope.

Colony formation assay

Cells were resuspended at a density of 400 cells per well in 6-well plates and allowed to grow at 37°C for 14 days. Colonies were then fixed and stained with crystal violet solution.

Wound-healing assay

Briefly, equal number of cells were seeded in 6-well plates and allowed to reach confluency. Several well-spanning scratches were made with a 10-μL pipette tip and culture medium was replaced with serum-free medium for further experimentation. Cell migration was observed at pre-marked positions below the wells using a Leica DMi8 inverted microscope at 100× magnifications.

Statistical analysis

Data are presented as the mean ± S.D. The results were analyzed with the one-way ANOVA test using GraphPad Prism software. Each experiment was carried out at least three times. Asterisks indicate that the values were significantly different from the control (*, $P < 0.05$; **, $P < 0.01$; ***, $P < 0.001$).

Results

EGCG treatment mediates ubiquitination and protein degradation of LATS1 and LATS2 in CRC cells

To investigate the effects of EGCG on the Hippo signaling pathway, we first evaluated EGCG-induced expression levels of Hippo pathway components in multiple CRC cell lines with western blot assays. In both HCT116 and RKO cells, EGCG treatment led to significantly decreased protein levels of total LATS1/2 and phosphorylated LATS1/2 in a dose- and time-dependent manner (**Figures 1A**, **1B** and S1A), as determined by immunoblotting with LATS1, LATS2, phospho-LATS1 (Thr1079) and phospho-LATS1 (Ser909) antibodies. Similar effects on total LATS1/2 and phosphorylated LATS1/2 were also observed in SW620 and LoVo CRC cell lines (Figure S1B and S1C). We also examined the effects of EGCG on endogenous WW45, MST1/2 and MOB1, which are upstream of LATS1/2. However, no significant changes were observed (Figure S1D). Interestingly, EGCG treatment did not significantly change the mRNA levels of LATS1/2 in HCT116 cells as determined by qPCR (Figure S1E). In addition, EGCG-mediated reductions in LATS1/2 were restored to control levels upon treatment with MG132, a proteasome inhibitor. However, the downregulation of LATS1/2 by EGCG was unaffected by treatment with NH_4Cl, a lysosome inhibitor, which indicates that EGCG may promote LATS1/2 ubiquitination (Figure S1F). Indeed, EGCG treatment increased the polyubiquitination levels of LATS1 and LATS2 in HEK293T cells (**Figure 1C** and **1D**).

Previous studies have shown that LATS1/2 are HSP90 clients and EGCG is a natural HSP90 inhibitor [31-33]. As a molecular chaperone, HSP90 typically promotes the stability of its client proteins. Thus we hypothesized that EGCG

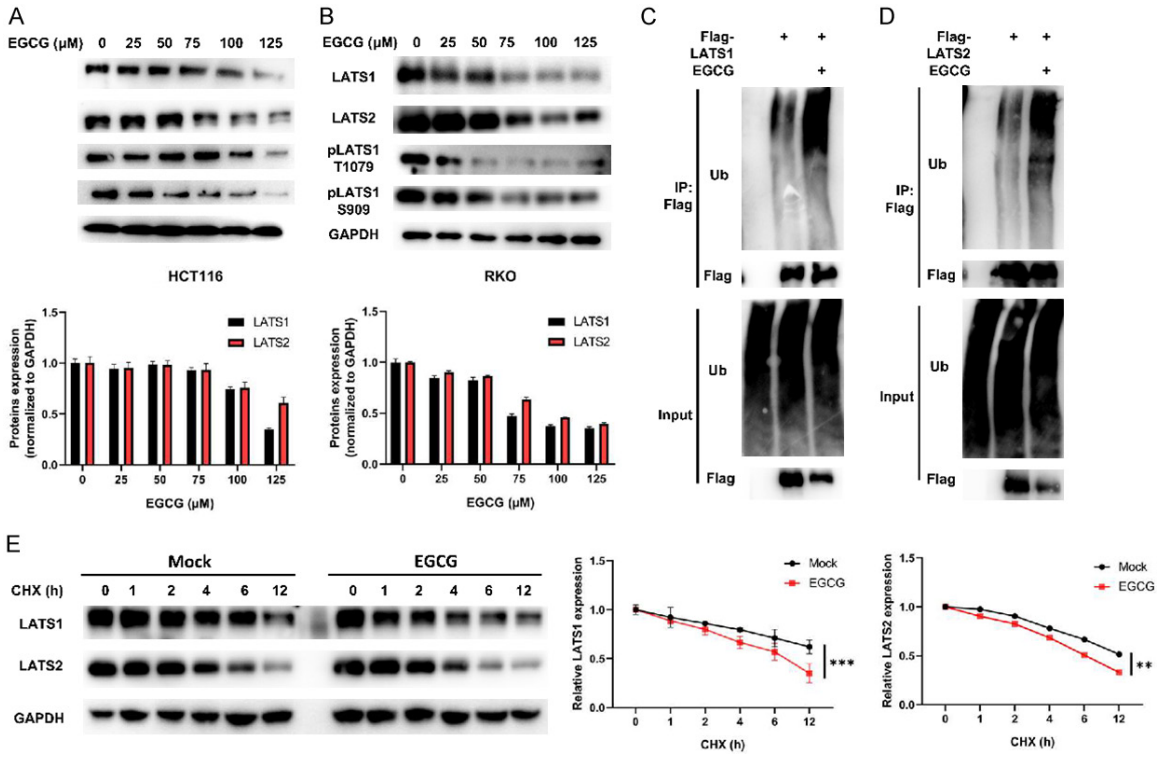

Figure 1. EGCG treatment mediates ubiquitination and protein degradation of LATS1 and LATS2 in colorectal cancer cells. (A) Subconfluent HCT116 cells were treated with EGCG at concentrations of 0, 25, 50, 75, 100 and 125 μM for 24 hr. After treatment, cell lysates were analyzed by immunoblotting (IB) for the indicated antigens. An example blot is shown on the upon. Data were expressed as mean ± SD of three independent experiments. (B) RKO cells were treated with different EGCG dose as in (A). Cell lysates were analyzed by immunoblotting for the indicated antigens. An example blot is shown on the upon, summary data on the bottom Data were expressed as mean ± SD of three independent experiments. (C and D) HCT116 cells were transfected with Flag-LATS1 (C) and Flag-LATS2 (D), 42 h post-transfection, cells were treated with 100 μM EGCG and 20 μM MG132 for another 6 h. Cell lysates were immunoprecipitated with anti-Flag antibody, followed by IB with indicated antibodies. (E) HCT116 cells were treated with EGCG in the absence or presence of cycloheximide (CHX, 0.05 mg/mL) for the indicated times, cell lysates were analyzed by immunoblotting for the expression of endogenous LATS1 and LATS2 proteins. Data were expressed as mean ± SD of three independent experiments.

regulates the protein stability of LATS1/2. Endogenous LATS1/2 turnover was faster in EGCG-treated samples than in mock-treated samples, when *de novo* protein synthesis was blocked by treatment with cycloheximide (CHX) (**Figure 1E**). Collectively, these results show that EGCG induces downregulation of LATS1/2 at protein and poly-ubiquitination levels in CRC cells.

CHIP interacts with and decreases LATS1/2 steady-state levels

HSP90 inhibition typically activates the E3 ubiquitin ligase CHIP, which works together with HSP70 to promote the ubiquitination and proteasomal and lysosomal degradation of misfolded or unfold HSP90 client proteins. Here, we found that EGCG indeed enhanced CHIP ubiquitin ligase activity (Figure S2A). Therefore, we speculated that CHIP may participate in the degradation of LATS1/2.

To test this hypothesis, we first examined whether CHIP physically interacts with LATS1/2. Ectopically expressed CHIP binds to LATS1 and LATS2 in HEK293T cells (**Figure 2A** and **2B**). Domain-mapping experiments revealed that CHIP associates with LATS1/2 via the tetratricopeptide repeat (TPR) domain (data not shown). Next, we tested whether CHIP affects the steady-state levels of LATS1/2. We observed that CHIP decreased LATS1 and LATS2 protein levels in HEK293T cells. In addition, CHIP-mediated reductions in LATS1/2 were restored to control levels upon treatment

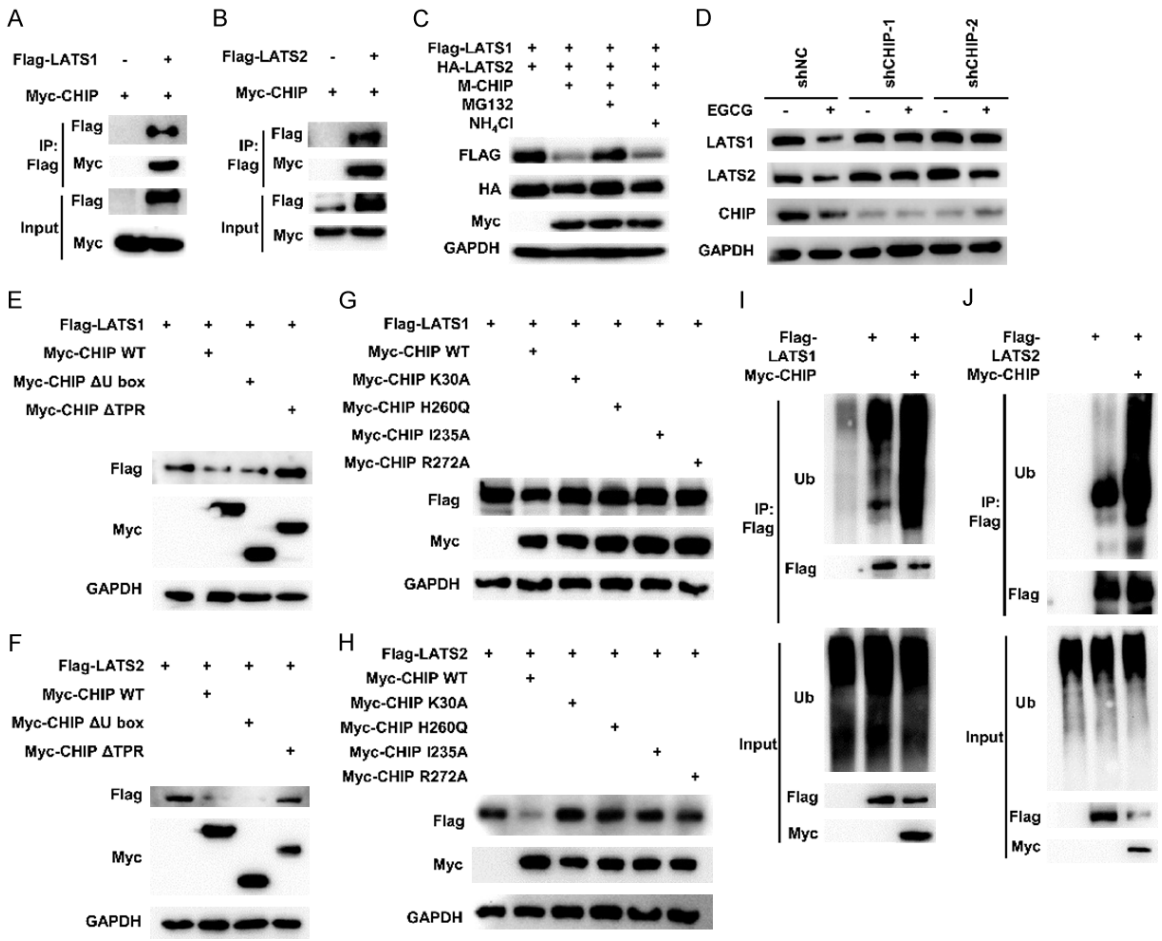

Figure 2. CHIP interacts with LATS1/2 and regulates LATS1/2 protein stability by mediating LATS1/2 ubiquitination. (A and B) Physical interaction between Flag-LATS1 and Myc-CHIP (A), Flag-LATS2 and Myc-CHIP (B) in HEK293T cells. Indicated plasmids were expressed in HEK293T cells, lysates were pulled-down with anti-Flag antibody followed by IB with indicated antibodies. (C) CHIP mediated LATS1/2 degradation mainly via the proteasome pathway. Flag-LATS1 and HA-LATS2 co-transfected with Myc-CHIP were expressed in HEK293T cells. 42 hr after transfection, cells were treated with 20 μM MG132 or 50 μM NH_4Cl for 6 hr and lysates were subjected to western blotting analysis. (D) Knockdown of CHIP upregulates LATS1/2 and block the down-regulation of LATS1/2 by EGCG. HEK293T cells were infected with either scrambled-shRNA or CHIP-shRNA lenti-viruses. EGCG treatment for 24 hr after 72 hr of infection. Endogenous LATS1, LATS2 and CHIP levels were detected by immunoblotting with indicated antibodies. (E and F) TPR domain of CHIP is required for CHIP mediated LATS1/2 downregulation. Flag-LATS1 (E) and Flag-LATS2 (F) co-transfected with Myc-CHIP WT or deletion mutants of CHIP (CHIPΔTPR, 135-303aa; CHIPΔU-box, 1-189aa) were expressed in HEK293T cells. Lysates were subjected to immunoblotting with indicated antibodies. (G and H) E3 ligase activity of CHIP is required for CHIP mediated LATS1/2 downregulation. Flag-LATS1 (G) and Flag-LATS2 (H) co-transfected with Myc-CHIP WT or point mutants of CHIP ($CHIP^{K30A}$, $CHIP^{H260Q}$, $CHIP^{I235A}$, $CHIP^{R272A}$) were expressed in HEK293T cells. Lysates were subjected to immunoblotting with indicated antibodies. (I and J) CHIP overexpression increases LATS1/2 ubiquitination. HCT116 were transfected with Flag-LATS1 (I) and Flag-LATS2 (J) with overexpressed Myc-CHIP WT. Cell lysates were immunoprecipitated with anti-Flag antibody, followed by IB with indicated antibodies.

with MG132. However, CHIP-mediated LATS1/2 downregulation was unaffected by treatment with NH_4Cl (**Figure 2C**). These results indicate that CHIP negatively regulates LATS1/2 levels through the proteasomal degradation pathway. Importantly, knockdown of CHIP enhanced the steady-state levels of endogenous LATS1/2 and inhibited their degradation by EGCG (**Figure 2D**). We then determined which region(s) of CHIP is/are critical for LATS1/2 degradation. First, CHIP TPR and U-box deletion mutants were used to map the specific region of CHIP required for LATS1/2 degradation. Our results showed that the CHIP TPR is necessary for

LATS1 and LATS2 degradation (**Figure 2E** and **2F**). Surprisingly, a CHIP U-box deletion mutant (lacking the E3 ligase U-box domain) was still able to decrease LATS1/2, as previously reported [34, 35]. Next, we generated CHIP constructs with point mutations and repeated this experiment. A K30A mutation in the CHIP TPR domain disrupts interactions with HSP70/90 chaperone proteins, whereas I235A, H260Q, and R272A mutations in the CHIP U-box domain all abolished its E3 ligase activity. WT CHIP, but not CHIP mutants (K30A, H260Q, I235A, and R272A) were found to decrease LATS1 and LATS2 (**Figure 2G** and **2H**).

Given that CHIP is an E3 ligase that physically associates with LATS1/2, we speculated that LATS1/2 may be poly-ubiquitinated by CHIP. We performed *in vivo* ubiquitination experiments by overexpressing Flag-tagged LATS1 or LATS2 and Myc-tagged CHIP in HEK293T cells. CHIP incorporated poly-ubiquitin chains into LATS1/2 (**Figure 2I** and **2J**). In contrast, LATS1/2 displayed decreased poly-ubiquitination when CHIP was knocked down (Figure S2B and S2C). On the basis of these data, we propose that CHIP-mediated poly-ubiquitination of LATS1/2 targets it for proteasomal degradation.

EGCG induces YAP hypo-phosphorylation, nuclear localization and activation in CRC cell lines

LATS1/2 is the major upstream kinase for YAP/TAZ phosphorylation, nuclear localization, and transcriptional coactivator activity. To investigate whether EGCG-mediated LATS1/2 reduction leads to YAP/TAZ hypo-phosphorylation, HCT116 cells were treated with EGCG. We observed that levels of endogenous YAP protein were moderately increased in a dose- and time-dependent manner. Additionally, Ser127 and Ser381, two major sites on YAP that are phosphorylated by LATS1/2, exhibited decreased phosphorylation levels, as detected by commercially available phospho-YAP specific antibodies (**Figures 3A** and S3A-C). Similar YAP and phospho-YAP trends were also observed in RKO cells (**Figures 3B**, S3D and S3E). Neither TAZ nor YAP mRNA levels changed in CRC cells in response to EGCG (Figure S3F). Phosphorylation at YAP Ser127 by LATS1/2 creates a binding motif for cytoplasmic protein 14-3-3, which promotes YAP cytoplasmic retention and inactivation. However, phosphorylation at YAP Ser381 by LATS1/2 produces a docking site for the E3 ligase beta-TrCP, which leads to YAP ubiquitination and degradation. We hypothesized that EGCG-mediated YAP Ser381 hypo-phosphorylation accounted for the observed YAP protein upregulation. To this hypothesis, we mutated all five LATS1/2 phosphorylation sites on YAP (YAP 5SA) [36] or constructed individual YAP S127A and YAP S381A mutations as previously described. Experiment with HCT116 cells, ectopically expressing YAP 5SA, YAP S127A, or YAP S381A showed that the YAP 5SA and YAP S381A phospho-resistant mutants ablated responses to EGCG (**Figure 3C**). We further analyzed the subcellular localization of overexpressed YAP in HCT116 cells by immunofluorescence. We found that a portion of YAP was translocated into the cell nucleus after EGCG treatment (**Figure 3D**). Nuclear-cytoplasmic fractionation assays in HCT116 cells further confirmed that EGCG treatment increased endogenous nuclear YAP levels (**Figure 3E**). Collectively, these results show that EGCG induces hypo-phosphorylation and nuclear localization of YAP in CRC cells.

We also investigated the effects of EGCG treatment on YAP transcriptional activity in CRC cells. Previous studies have shown that dephosphorylated YAP binds to TEAD transcription factors to promote transcription of target genes such as *CTGF* and *CYR61* [37-39]. The compound Verteporfin (VP) reportedly specifically disrupts YAP-TEADs interactions, thus inhibiting YAP-TEADs complex formation and transcriptional activity. Therefore, we examined the expression of YAP target genes in response to EGCG. In HCT116 and RKO cells, EGCG treatment significantly induced the expression of *CTGF*, *CYR61* and *ANKRD1*, whereas VP partially blocked their upregulation (**Figures 3F** and S4A). We also examined the effect of EGCG treatment on YAP transcriptional activity using the previously described 8xGTIIC-luciferase reporter [40]. EGCG strongly induced YAP activation on the synthetic promoter of the 8xGTIIC-luciferase reporter, which was alleviated by VP treatment (**Figure 3G**). In order to further study the relationship between YAP and EGCG treatment, we generated HCT116 and RKO cells with stable YAP knockdown (Figure S4B and S4C). EGCG-induced expression of *CTGF*, *CYR61* and *ANKRD1* was substantially reduced

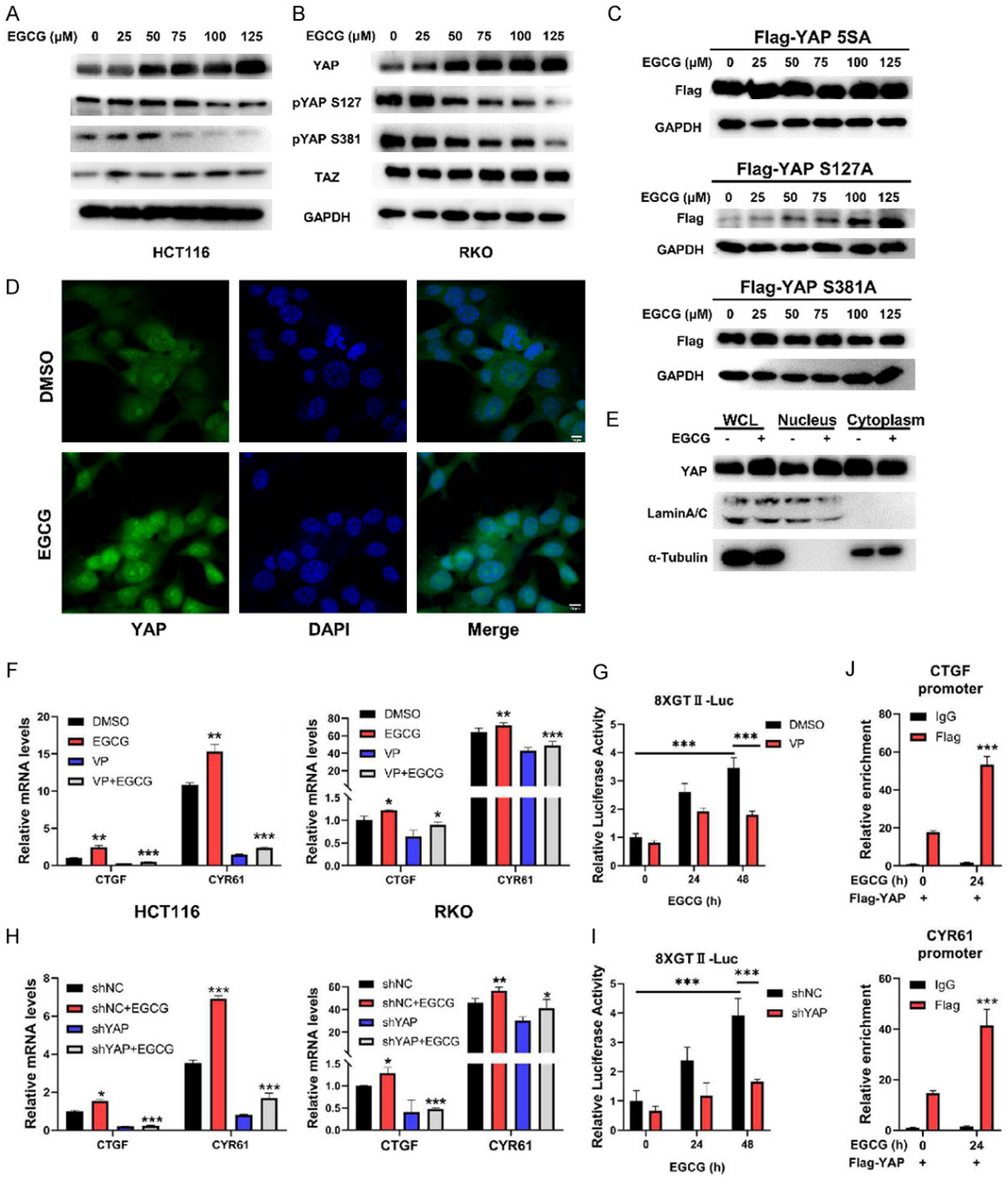

Figure 3. EGCG upregulates the nuclear translocation and transcriptional activity of YAP in colorectal cancer cells. (A, B) Subconfluent HCT116 (A) cells or RKO cells (B) were treated with EGCG at concentrations of 0, 25, 50, 75, 100 and 125 μM for 24 hr. After treatment, cell lysates were analyzed by immunoblotting for the indicated antigens. (C) HCT116 cells were transfected with Flag-YAP 5SA, Flag-YAP S127A, or Flag-YAP S381A mutants, EGCG treatment was performed as the same as in (A), cell lysates were prepared for immunoblotting with the indicated antibodies. (D, E) HCT116 cells were treated with solvent or EGCG for 24 hr, the subcellular localization of YAP was detected by immunofluorescence (IF) analysis (D) and nuclear-cytoplasmic fractionation assay (E) with the indicated antibodies. (F) HCT116 and RKO cells were treated with solvent or Verteporfin (VP, a specific YAP-TEAD inhibitor) in combination with or without EGCG (75 μM) for 24 hr, mRNA expression of CTGF and CYR61 were detected by qPCR. (G) HCT116 cell were co-transfected with YAP responsive reporter 8xGTIIC-luciferase and Renilla and treated with solvent or VP in combination with or without EGCG (75 μM) for the indicated times, dual luciferase reporter assay were performed to quantify YAP transcriptional activities. (H) shNC and shYAP HCT116 or RKO cells were treated with EGCG (75 μM) for 24 hr, CTGF and CYR61 mRNA levels were analysed by qPCR. (I) shNC and shYAP HCT116 cell clones were

co-transfected with YAP responsive reporter 8xGTIIC-luciferase and Renilla and were treated with EGCG (75 μM) for the indicated times, dual luciferase reporter assay was performed to quantify YAP transcriptional activities. (J) YAP overexpression HCT116 cells were firstly treated with EGCG (75 μM) for 24 hr, chromatin immunoprecipitation assay confirmed that EGCG treatment increased YAP binding on CTGF and CYR61 promoter.

under these conditions (**Figures 3H** and S4D). Similarly, YAP knockdown mitigated EGCG-induced YAP-mediated activation of the 8xGTIIC-luciferase reporter (**Figure 3I**). ChIP assays showed that EGCG-mediated *CTGF* and *CYR61* expression was at least partially dependent on YAP (**Figure 3J**). Collectively, these data indicate that EGCG induces YAP hypo-phosphorylation, nuclear translocation and transcriptional activation in CRC cell lines.

YAP knockdown sensitizes CRC cells to EGCG partially by decreasing cell proliferation

LATS1/2 are classic tumor suppressors while YAP usually functions as an oncoprotein. In many cancers, YAP promotes tumorigenesis through multiple mechanisms such as acceleration of cell cycle progression. In the current study, we hypothesized that EGCG mediated LATS1/2 degradation and YAP activation in CRC cells could counteract the tumor-suppressive role of EGCG in cell cycle regulation. If true, knockdown of YAP in CRC cells would increase the anti-tumor activities of EGCG. Therefore, cell viability was assessed with the MTT assay, EdU labeling, colony formation analysis and cell cycle analysis. In both HCT116 and RKO cell lines, MTT and colony formation assays showed that cell growth was decreased by combined treatment with EGCG and YAP shRNA (**Figure 4A-D**). We further investigated the effect of EGCG on the cell cycle distribution of RKO cells stably expressing shYAP or a negative control shRNA (shNC). Flow cytometric cell cycle analysis revealed that combined YAP knockdown and EGCG treatment induced CRC cell accumulation in sub-G0/G1 phase and reduced cells in S phase, with little change in G2 phase (**Figure 4E**). Consistently, the number of EdU-positive cells following combined treatment with EGCG and shYAP was substantially smaller than that in the groups treated with YAP shRNA or EGCG alone (**Figure 4F**). Altogether, these results indicate that YAP silencing combined with EGCG treatment decreases CRC cell proliferation.

YAP knockdown sensitizes CRC cells to EGCG partially by promoting cell apoptosis

YAP downregulation promotes apoptosis by affecting multiple biological processes, including the accumulation of ROS [41]. To demonstrate the impact of combined EGCG treatment and YAP knockdown on ROS generation in CRC cells, ROS was detected using DCFH-DA, a fluorescent dye. Fluorescence intensity is proportional to ROS levels. RKO cells with both YAP knockdown and EGGC treatment exhibited stronger fluorescence signal than RKO cells treated only with EGGC (without YAP knockdown) (**Figure 5A**). Similar results were observed in HCT116 cells (**Figure 5B**). In addition, flow cytometry revealed that RKO cells with both EGCG-treatment and YAP knockdown were more apoptotic than control RKO cells (**Figure 5C**). In summary, EGCG-induced YAP activation plays an important role in anti-apoptosis. Additionally, knockdown of YAP enhances the anti-tumor activities of EGCG in CRC cells at least partially through inhibiting cell proliferation and promoting cell apoptosis.

Downregulation of YAP sensitizes CRC cells to EGCG partially through modulation of the epithelial-mesenchymal transition (EMT) and MDR gene expression

Both EMT and MDR can be involved in tumor progression and recurrence. Of interest, YAP can directly or indirectly affect these biological processes [42-46]. Therefore, we analyzed changes in wound-healing behavior, EMT markers expression and MDR gene expression levels. The wound-healing experiments showed that the migratory capacity of shYAP RKO cells was significantly reduced in response to EGCG treatment, when compared to shNC+EGCG RKO cells (**Figure 6A**). Accordingly, shYAP combined with EGCG enhanced the expression of E-cadherin and ZO-3, but suppressed the expression of mesenchymal marker genes (N-cadherin and vimentin), the EMT transcription factors Snail and Slug, in HCT116 and RKO cells (**Figure 6B** and **6C**). Similarly, while EGCG treatment slightly increased the expression of some MDR genes, such as *ABCB1*, *ABCC1*, and *ABCG2*, EGCG treatment in YAP knockdown RKO and HCT116 cells reduced *ABCB1* and *ABCC1* expression (**Figure 6D** and **6E**). These results suggest that EGCG mediated YAP activation in CRC cells antagonizes the therapeutic

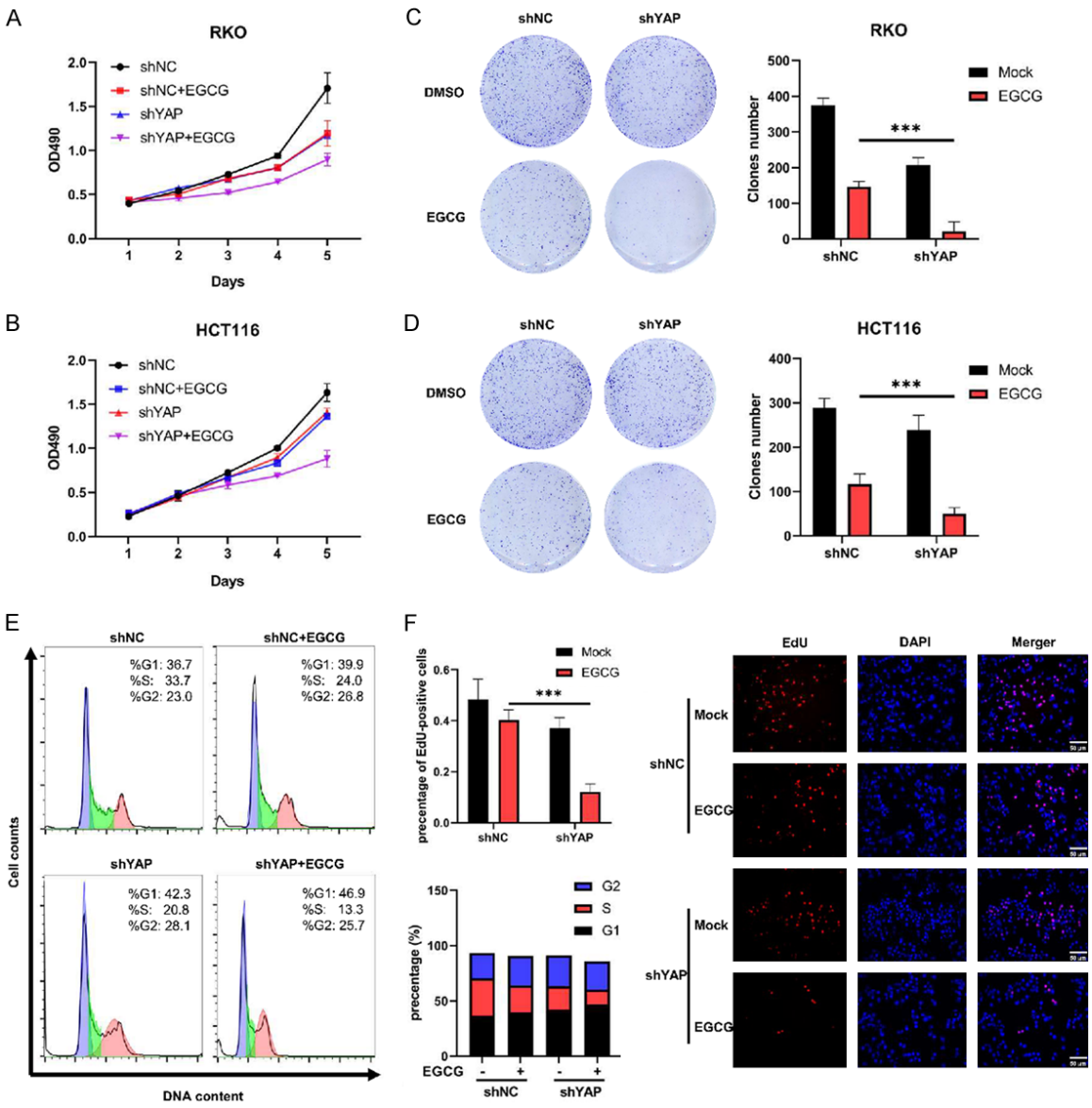

Figure 4. YAP knockdown sensitizes colorectal cancer cells to EGCG partly through decreased cell proliferation. (A and B) Stable knockdown RKO cell lines (A) or HCT116 cell lines (B) with shYAP and shNC were exposed to EGCG (50 μM) and cell proliferation was measured by MTT assay at the indicated time points. (C and D) Stable knockdown RKO cell lines (C) or HCT116 cell lines (D) with shYAP and shNC were treated with EGCG (50 μM) for two weeks, colony formation assay was performed to evaluate the clonogenic ability of cells. Cells were stained by crystal violet in the left panel and quantified in the right panel. (E) RKO cells were treated with EGCG (50 μM) for 24 hr, and cell cycle distribution was analyzed by flow cytometry. Representative flow cytograms are shown in the left panel. (F) Proliferation in shNC or shYAP RKO cells in (A) was detected using the EdU assay and fluorescence microscope after treated with EGCG (50 μM) for 24 hr. Representative picture as shown in the right panel. All assays were performed in triplicate and repeated three times.

effect of EGCG at least partially through EMT and drug efflux pumps.

Discussion

Resistance to chemotherapy, tumor recurrence, and side effect-induced treatment interruption, are major problems in CRC treatment. Combining traditional anti-neoplastic drugs with bioactive plant-derived primary or secondary metabolites has been an active area of research in recent years. These combination therapy strategies have been demonstrated to exert additive or synergistic effects on cancer

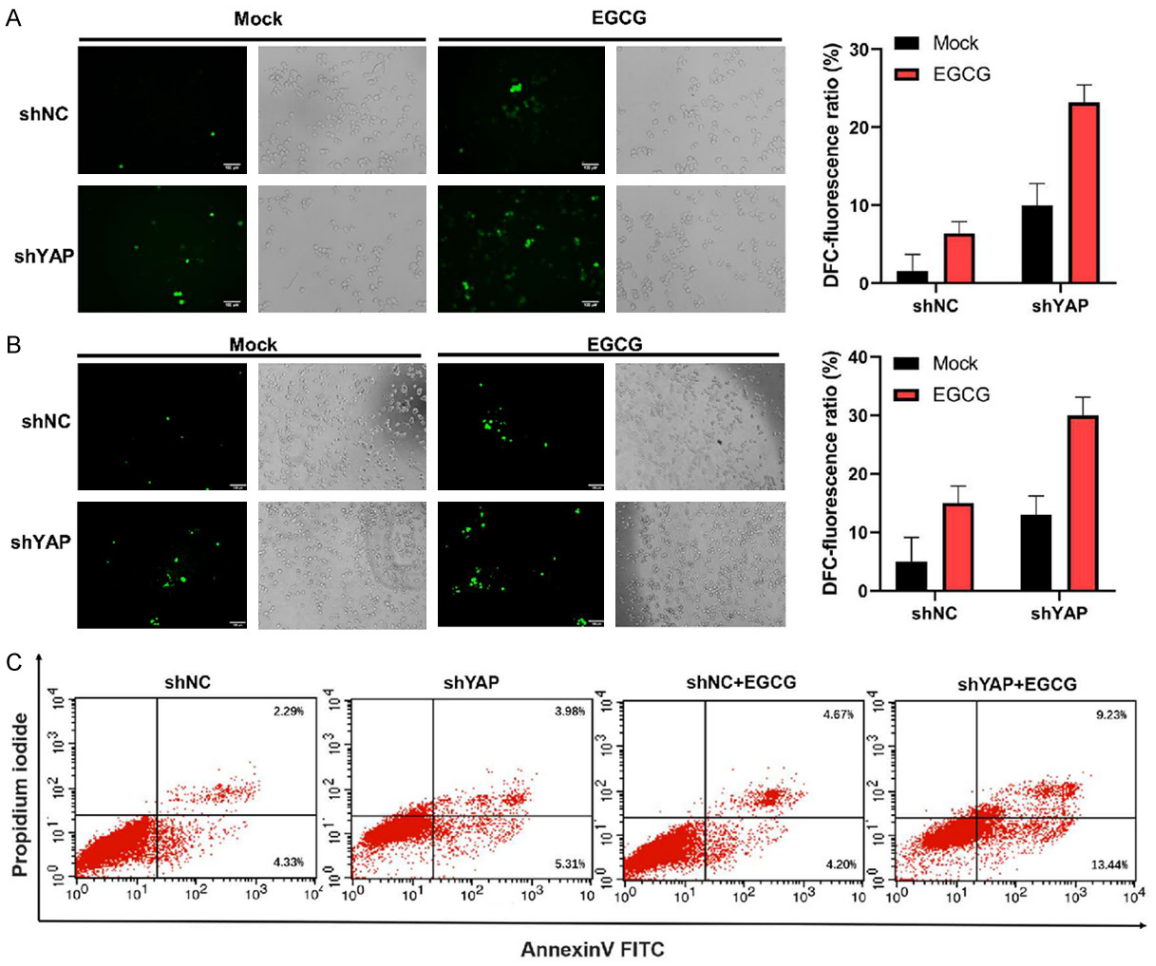

Figure 5. YAP knockdown sensitizes colorectal cancer cells to EGCG partly through increased cell apoptosis. (A and B) ShNC or shYAP RKO cells (A) or HCT116 cells (B) were treated with or without EGCG (50 μM) for 24 hr. The contents of ROS were measured using an inverted fluorescence microscope using the DCFH-DA fluorescent dye. Representative photographs (left), and the corresponding cumulative data (right). Data were expressed as mean ± SD of three independent experiments. (C) Flow cytometric analysis of shNC or shYAP RKO cells were treated with or without EGCG (50 μM) for 24 hr, Flow cytometry profile represented FITC-Annexin V staining on the X axis and PI on the Y axis.

prevention and minimize treatment-induced toxicity. EGCG, a compound from green tea, can inhibit the proliferation of over 20 different cancer lines cell [47]. In the current study, we systematically investigated the effects and molecular mechanisms of EGCG on Hippo signaling transduction in CRC cells. We report that in CRC cells exposed to EGCG, the core Hippo signaling pathway kinase LATS1/2 is ubiquitinated by the E3 ligase CHIP and degraded by the proteasome. Additionally, the downstream effector YAP translocates to nucleus and trans-activates the expression of critical YAP target genes, ultimately antagonizing the anti-tumor effects of EGCG in CRC cell (**Figure 6F**).

YAP is believed to be an oncoprotein that is hyperactivated in many caner types where it contribute to the tumorigenesis and recurrence [42]. We found that EGCG activates YAP in CRC cells. Similarly, other drugs such as doxorubicin, 5-fluorouracil, and Taxol can also lead to YAP nuclear translocation and activity to a certain extent [48-50]. Moreover, YAP expression levels are positively correlated with colon cancer liver metastasis and recurrence after chemotherapy [49]. Although the upstream mechanisms are different, these data suggest that YAP activation is the cause of chemotherapy paradoxically promoting tumor cell survival/proliferation. Research is clearly needed to fur-

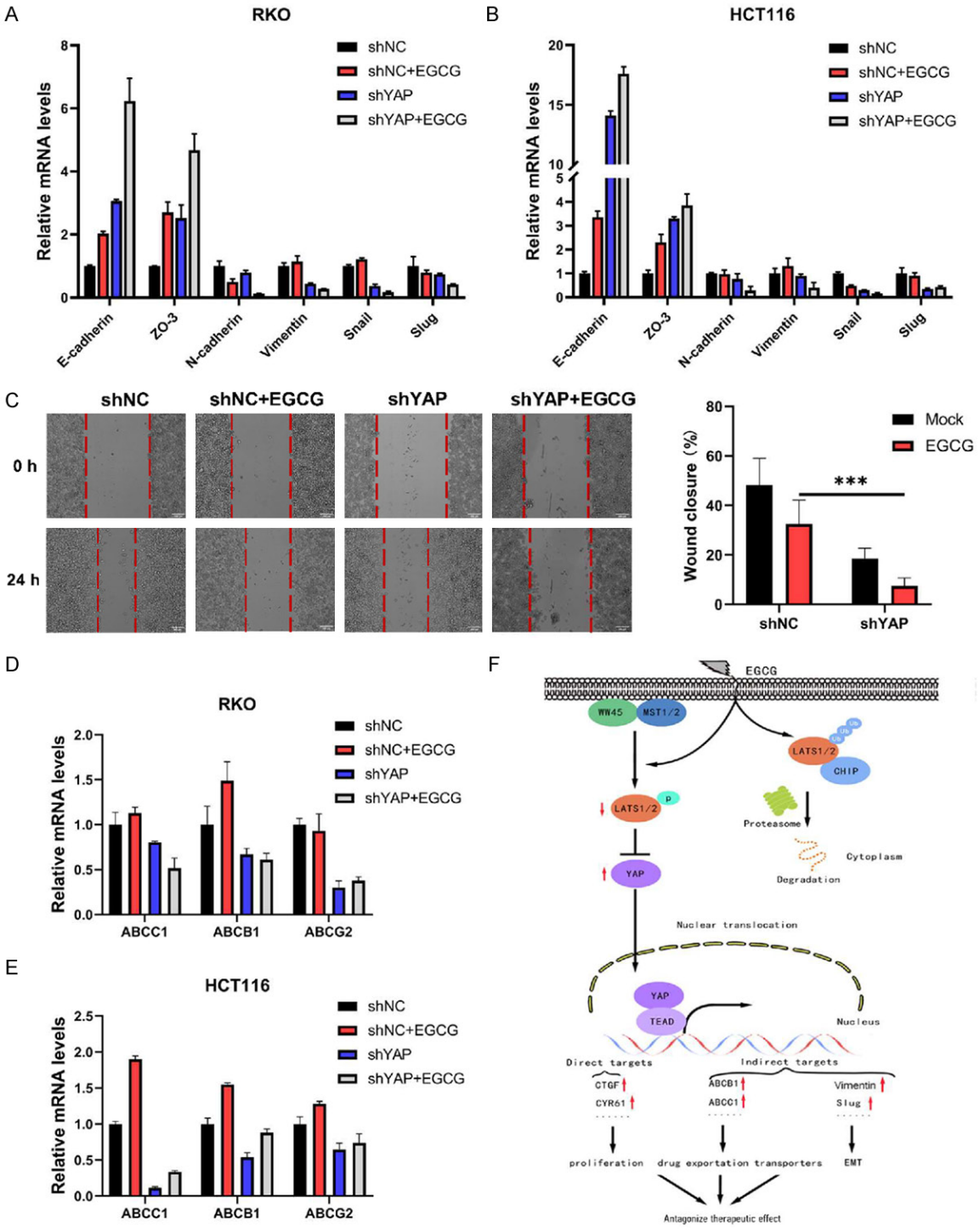

Figure 6. Downregulation of YAP sensitizes colorectal cancer cells to EGCG partially through modulation of the epithelial mesenchymal transition and Multi Drug Resistance gene expression. (A and B) ShNC and shYAP RKO cells (A) or HCT116 cells (B) were treated with EGCG (75 μM) for 24 hr, E-cadherin, ZO-3, N-cadherin, Vimentin, Snail and Slug mRNA levels were analyzed by qPCR. (C) The cell migration capacity of the stable knockdown RKO cell lines with shYAP and shNC was analyzed by using scratch assay following treatment with EGCG (50 μM) for 24 hr (magnification, ×100) and the percentage of wound closure was statistically analyzed. (D and E) ShNC and shYAP RKO cells (D) or HCT116 cells (E) were treated with EGCG (75 μM) for 24 hr, ABCC1, ABCB1 and ABCG2 mRNA levels were analyzed by qPCR. (F) This model describes the key role of YAP in antagonizing EGCG treatment in CRC cells.

ther demonstrate this paradox, since improving chemotherapy's effectiveness against tumors is crucial. At the same time, Hippo-LATS based tumor-suppressive pathway may play an important role in improving anti-tumor effect [51-53]. Therefore, it will be interesting to investigate whether and how YAP and other components of the Hippo-LATS pathway interact to improve anti-tumor effect.

Several recent reports have shown that EGCG has strong anti-cancer activity and can inhibit the PI3K-Akt and EGFR signal transduction pathway and up-regulation of TP53 expression [54-56]. However, the anti-tumor effects of EGCG are still controversial in clinical contexts. For example, due to the instability and rapid metabolism of EGCG and its derivatives [57], it is difficult to maintain effective local concentration of EGCG in tumors. EGCG is also less potent than conventional anti-cancer drugs; previous studies have shown that it is approximately 250-fold less effective than Adriamycin in lung cancer cell lines [58]. Additionally, EGCG may not completely eradicate tumor cells or maintain its effects, indicating that it may promote the emergence and enrichment of drug-resistant tumor cell subsets. This factor may lead to unsatisfactory clinical outcomes following EGCG treatment. To address this dilemma, two options exist including long-term high-dose EGCG therapy and administration of EGCG together with other drugs. However, high doses of EGCG triggers a series of side effects. Phase I and II clinical studies have found that side effect of EGCG use include hepatotoxicity, nausea, insomnia, abdominal pain, and diarrhea, among others [59-61]. Therefore, combining EGCG with other drugs may be a better strategy to restore drug sensitivity and balance cytotoxicity. In our study, YAP may be a potential target for reversing the EGCG sensitivity in CRC cells; combine EGCG treatment and inhibition of YAP activity may improve anti-tumor effects. Many YAP inhibitors are currently in clinical trials, and more clinical trials are clearly needed to evaluate the anti-tumor efficacy and side effects of EGCG combined with various doses and types of YAP inhibitors.

Overall, our results suggest that inhibition of YAP activity in CRC can be used in combination with EGGC to improve anti-tumor effects. This study expanded our understanding on the role of YAP in the antagonism of tumor therapy and provided a theoretical basis for the further discovery and utilization of EGCG in the clinic.

Acknowledgements

We thank Wang-Lai Hu and Su-Mei Zhang for all their invaluable efforts and technical assistance. This research was funded by the National Natural Science Foundation of China (Grant No. 31571506 and No. 32070616), the Open Fundamental Research Funds from the State Key Laboratory of Tea Plant Biology and Utilization (SKLTOF20180102) and the Universities Natural Science Research Project of Anhui Province (KJ2018A0140).

Disclosure of conflict of interest

None.

Address correspondence to: Shou-Jun Huang, School of Life Sciences, Anhui Agricultural University, 130 West Changjiang Road, Hefei 230036, Anhui, China. Tel: +86-18788877198; E-mail: huangshoujun@ahau.edu.cn; Zhong-Wen Xie, State Key Laboratory of Tea Plant Biology and Utilization, Anhui Agricultural University, 130 West Changjiang Road, Hefei 230036, Anhui, China. Tel: +86-18856-088327; E-mail: zhongwenxie@ahau.edu.cn

References

[1] Bray F, Ferlay J, Soerjomataram I, Siegel RL, Torre LA and Jemal A. Global cancer statistics 2018: GLOBOCAN estimates of incidence and mortality worldwide for 36 cancers in 185 countries. CA Cancer J Clin 2018; 68: 394-424.

[2] Arnold M, Sierra MS, Laversanne M, Soerjomataram I, Jemal A and Bray F. Global patterns and trends in colorectal cancer incidence and mortality. Gut 2017; 66: 683-691.

[3] Leslie A, Carey FA, Pratt NR and Steele RJ. The colorectal adenoma-carcinoma sequence. Br J Surg 2002; 89: 845-860.

[4] Nguyen HT and Duong HQ. The molecular characteristics of colorectal cancer: Implications for diagnosis and therapy. Oncol Lett 2018; 16: 9-18.

[5] Simon K. Colorectal cancer development and advances in screening. Clin Interv Aging 2016; 11: 967-976.

[6] Kunjachan S, Rychlik B, Storm G, Kiessling F and Lammers T. Multidrug resistance: physiological principles and nanomedical solutions. Adv Drug Deliv Rev 2013; 65: 1852-1865.

[7] Wang YJ, Zhang YK, Zhang GN, Al Rihani SB, Wei MN, Gupta P, Zhang XY, Shukla S, Ambudkar SV, Kaddoumi A, Shi Z and Chen ZS. Regorafenib overcomes chemotherapeutic multidrug resistance mediated by ABCB1 transporter in colorectal cancer: in vitro and in vivo study. Cancer Lett 2017; 396: 145-154.
[8] Yu FX, Zhao B and Guan KL. Hippo pathway in organ size control, tissue homeostasis, and cancer. Cell 2015; 163: 811-828.
[9] Moroishi T, Hansen CG and Guan KL. The emerging roles of YAP and TAZ in cancer. Nat Rev Cancer 2015; 15: 73-79.
[10] Lei QY, Zhang H, Zhao B, Zha ZY, Bai F, Pei XH, Zhao S, Xiong Y and Guan KL. TAZ promotes cell proliferation and epithelial-mesenchymal transition and is inhibited by the Hippo pathway. Mol Cell Biol 2008; 28: 2426-2436.
[11] Zhao B, Wei X, Li W, Udan RS, Yang Q, Kim J, Xie J, Ikenoue T, Yu J, Li L, Zheng P, Ye K, Chinnaiyan A, Halder G, Lai ZC and Guan KL. Inactivation of YAP oncoprotein by the Hippo pathway is involved in cell contact inhibition and tissue growth control. Genes Dev 2007; 21: 2747-2761.
[12] Liu CY, Zha ZY, Zhou X, Zhang H, Huang W, Zhao D, Li T, Chan SW, Lim CJ, Hong W, Zhao S, Xiong Y, Lei QY and Guan KL. The Hippo tumor pathway promotes TAZ degradation by phosphorylating a phosphodegron and recruiting the SCF{beta}-TrCP E3 ligase. J Biol Chem 2010; 285: 37159-37169.
[13] Zhao B, Li L, Tumaneng K, Wang CY and Guan KL. A coordinated phosphorylation by Lats and CK1 regulates YAP stability through SCF(beta-TRCP). Genes Dev 2010; 24: 72-85.
[14] Moon S, Yeon Park S and Woo Park H. Regulation of the Hippo pathway in cancer biology. Cell Mol Life Sci 2018; 75: 2303-2319.
[15] Guo PD, Lu XX, Gan WJ, Li XM, He XS, Zhang S, Ji QH, Zhou F, Cao Y, Wang JR, Li JM and Wu H. RARγ downregulation contributes to colorectal tumorigenesis and metastasis by derepressing the Hippo-Yap pathway. Cancer Res 2016; 76: 3813-3825.
[16] Hall CA, Wang R, Miao J, Oliva E, Shen X, Wheeler T, Hilsenbeck SG, Orsulic S and Goode S. Hippo pathway effector Yap is an ovarian cancer oncogene. Cancer Res 2010; 70: 8517-8525.
[17] Zhang X, Zhao H, Li Y, Xia D, Yang L, Ma Y and Li H. The role of YAP/TAZ activity in cancer metabolic reprogramming. Mol Cancer 2018; 17: 134.
[18] Greenberg JA, Axen KV, Schnoll R and Boozer CN. Coffee, tea and diabetes: the role of weight loss and caffeine. Int J Obes (Lond) 2005; 29: 1121-1129.
[19] Cabrera C, Artacho R and Giménez R. Beneficial effects of green tea--a review. J Am Coll Nutr 2006; 25: 79-99.
[20] Chacko SM, Thambi PT, Kuttan R and Nishigaki I. Beneficial effects of green tea: a literature review. Chin Med 2010; 5: 13.
[21] Sourabh A, Kanwar SS, Sud RG, Ghabru A and Sharma OP. Influence of phenolic compounds of Kangra tea [Camellia sinensis (L) O Kuntze] on bacterial pathogens and indigenous bacterial probiotics of Western Himalayas. Braz J Microbiol 2014; 44: 709-715.
[22] Sinha D, Biswas J, Nabavi SM and Bishayee A. Tea phytochemicals for breast cancer prevention and intervention: from bench to bedside and beyond. Semin Cancer Biol 2017; 46: 33-54.
[23] Rawangkan A, Wongsirisin P, Namiki K, Iida K, Kobayashi Y, Shimizu Y, Fujiki H and Suganuma M. Green tea catechin is an alternative immune checkpoint inhibitor that inhibits PD-L1 expression and lung tumor growth. Molecules 2018; 23: 2071.
[24] Lai YH, Sun CP, Huang HC, Chen JC, Liu HK and Huang C. Epigallocatechin gallate inhibits hepatitis B virus infection in human liver chimeric mice. BMC Complement Altern Med 2018; 18: 248.
[25] Shin CM, Lee DH, Seo AY, Lee HJ, Kim SB, Son WC, Kim YK, Lee SJ, Park SH, Kim N, Park YS and Yoon H. Green tea extracts for the prevention of metachronous colorectal polyps among patients who underwent endoscopic removal of colorectal adenomas: a randomized clinical trial. Clin Nutr 2018; 37: 452-458.
[26] Roowi S, Stalmach A, Mullen W, Lean ME, Edwards CA and Crozier A. Green tea flavan-3-ols: colonic degradation and urinary excretion of catabolites by humans. J Agric Food Chem 2010; 58: 1296-1304.
[27] Saldanha SN, Kala R and Tollefsbol TO. Molecular mechanisms for inhibition of colon cancer cells by combined epigenetic-modulating epigallocatechin gallate and sodium butyrate. Exp Cell Res 2014; 324: 40-53.
[28] Kumazoe M, Sugihara K, Tsukamoto S, Huang Y, Tsurudome Y, Suzuki T, Suemasu Y, Ueda N, Yamashita S, Kim Y, Yamada K and Tachibana H. 67-kDa laminin receptor increases cGMP to induce cancer-selective apoptosis. J Clin Invest 2013; 123: 787-799.
[29] Sukhthankar M, Yamaguchi K, Lee SH, McEntee MF, Eling TE, Hara Y and Baek SJ. A green tea component suppresses posttranslational expression of basic fibroblast growth factor in colorectal cancer. Gastroenterology 2008; 134: 1972-1980.
[30] Pahlke G, Ngiewih Y, Kern M, Jakobs S, Marko D and Eisenbrand G. Impact of quercetin and

EGCG on key elements of the Wnt pathway in human colon carcinoma cells. J Agric Food Chem 2006; 54: 7075-7082.
[31] Huntoon CJ, Nye MD, Geng L, Peterson KL, Flatten KS, Haluska P, Kaufmann SH and Karnitz LM. Heat shock protein 90 inhibition depletes LATS1 and LATS2, two regulators of the mammalian Hippo tumor suppressor pathway. Cancer Res 2010; 70: 8642-8650.
[32] Moses MA, Henry EC, Ricke WA and Gasiewicz TA. The heat shock protein 90 inhibitor, (-)-epigallocatechin gallate, has anticancer activity in a novel human prostate cancer progression model. Cancer Prev Res (Phila) 2015; 8: 249-257.
[33] Iqbal MK, Liu J, Nabi F, Rehman MU, Zhang H, Tahir AH and Li J. Recovery of chicken growth plate by heat-shock protein 90 inhibitors epigallocatechin-3-gallate and apigenin in thiram-induced tibial dyschondroplasia. Avian Dis 2016; 60: 773-778.
[34] Li X, Huang M, Zheng H, Wang Y, Ren F, Shang Y, Zhai Y, Irwin DM, Shi Y, Chen D and Chang Z. CHIP promotes Runx2 degradation and negatively regulates osteoblast differentiation. J Cell Biol 2008; 181: 959-972.
[35] Paul I, Ahmed SF, Bhowmik A, Deb S and Ghosh MK. The ubiquitin ligase CHIP regulates c-Myc stability and transcriptional activity. Oncogene 2013; 32: 1284-1295.
[36] Moroishi T, Hayashi T, Pan WW, Fujita Y, Holt MV, Qin J, Carson DA and Guan KL. The Hippo pathway kinases LATS1/2 suppress cancer immunity. Cell 2016; 167: 1525-1539, e17.
[37] Zhou Y, Huang T, Cheng AS, Yu J, Kang W and To KF. The TEAD family and its oncogenic role in promoting tumorigenesis. Int J Mol Sci 2016; 17: 138.
[38] Zhao B, Ye X, Yu J, Li L, Li W, Li S, Yu J, Lin JD, Wang CY, Chinnaiyan AM, Lai ZC and Guan KL. TEAD mediates YAP-dependent gene induction and growth control. Genes Dev 2008; 22: 1962-1971.
[39] Zhang H, Liu CY, Zha ZY, Zhao B, Yao J, Zhao S, Xiong Y, Lei QY and Guan KL. TEAD transcription factors mediate the function of TAZ in cell growth and epithelial-mesenchymal transition. J Biol Chem 2009; 284: 13355-13362.
[40] Dupont S, Morsut L, Aragona M, Enzo E, Giulitti S, Cordenonsi M, Zanconato F, Le Digabel J, Forcato M, Bicciato S, Elvassore N and Piccolo S. Role of YAP/TAZ in mechanotransduction. Nature 2011; 474: 179-183.
[41] Wang M, Dong Y, Gao S, Zhong Z, Cheng C, Qiang R, Zhang Y, Shi X, Qian X, Gao X, Guan B, Yu C, Yu Y and Chai R. Hippo/YAP signaling pathway protects against neomycin-induced hair cell damage in the mouse cochlea. Cell Mol Life Sci 2022; 79: 79.
[42] Zanconato F, Cordenonsi M and Piccolo S. YAP/TAZ at the roots of cancer. Cancer Cell 2016; 29: 783-803.
[43] Reggiani F, Gobbi G, Ciarrocchi A, Ambrosetti DC and Sancisi V. Multiple roles and context-specific mechanisms underlying YAP and TAZ-mediated resistance to anti-cancer therapy. Biochim Biophys Acta Rev Cancer 2020; 1873: 188341.
[44] Shao DD, Xue W, Krall EB, Bhutkar A, Piccioni F, Wang X, Schinzel AC, Sood S, Rosenbluh J, Kim JW, Zwang Y, Roberts TM, Root DE, Jacks T and Hahn WC. KRAS and YAP1 converge to regulate EMT and tumor survival. Cell 2014; 158: 171-184.
[45] Suemura S, Kodama T, Myojin Y, Yamada R, Shigekawa M, Hikita H, Sakamori R, Tatsumi T and Takehara T. CRISPR loss-of-function screen identifies the Hippo signaling pathway as the mediator of regorafenib efficacy in hepatocellular carcinoma. Cancers (Basel) 2019; 11: 1362.
[46] Liu X, Chen J, Li W, Hang C and Dai Y. Inhibition of casein kinase II by CX-4945, but not yes-associated protein (YAP) by verteporfin, enhances the antitumor efficacy of temozolomide in glioblastoma. Transl Oncol 2020; 13: 70-78.
[47] Chen D, Wan SB, Yang H, Yuan J, Chan TH and Dou QP. EGCG, green tea polyphenols and their synthetic analogs and prodrugs for human cancer prevention and treatment. Adv Clin Chem 2011; 53: 155-177.
[48] Ma K, Xu Q, Wang S, Zhang W, Liu M, Liang S, Zhu H and Xu N. Nuclear accumulation of yes-associated protein (YAP) maintains the survival of doxorubicin-induced senescent cells by promoting survivin expression. Cancer Lett 2016; 375: 84-91.
[49] Touil Y, Igoudjil W, Corvaisier M, Dessein AF, Vandomme J, Monté D, Stechly L, Skrypek N, Langlois C, Grard G, Millet G, Leteurtre E, Dumont P, Truant S, Pruvot FR, Hebbar M, Fan F, Ellis LM, Formstecher P, Van Seuningen I, Gespach C, Polakowska R and Huet G. Colon cancer cells escape 5FU chemotherapy-induced cell death by entering stemness and quiescence associated with the c-Yes/YAP axis. Clin Cancer Res 2014; 20: 837-846.
[50] Lai D, Ho KC, Hao Y and Yang X. Taxol resistance in breast cancer cells is mediated by the Hippo pathway component TAZ and its downstream transcriptional targets Cyr61 and CTGF. Cancer Res 2011; 71: 2728-2738.
[51] Visser S and Yang X. Identification of LATS transcriptional targets in HeLa cells using whole human genome oligonucleotide microarray. Gene 2010; 449: 22-29.
[52] Zhao QZ and Dou KF. Methylation of Ras association domain family protein 1, isoform a

correlated with proliferation and drug resistance in hepatocellular carcinoma cell line SMMC-7721. J Gastroenterol Hepatol 2007; 22: 683-689.
[53] Ren A, Yan G, You B and Sun J. Down-regulation of mammalian sterile 20-like kinase 1 by heat shock protein 70 mediates cisplatin resistance in prostate cancer cells. Cancer Res 2008; 68: 2266-2274.
[54] Liu S, Wang XJ, Liu Y and Cui YF. PI3K/AKT/mTOR signaling is involved in (-)-epigallocatechin-3-gallate-induced apoptosis of human pancreatic carcinoma cells. Am J Chin Med 2013; 41: 629-642.
[55] Pan MH, Lin CC, Lin JK and Chen WJ. Tea polyphenol (-)-epigallocatechin 3-gallate suppresses heregulin-beta1-induced fatty acid synthase expression in human breast cancer cells by inhibiting phosphatidylinositol 3-kinase/Akt and mitogen-activated protein kinase cascade signaling. J Agric Food Chem 2007; 55: 5030-5037.
[56] Hastak K, Gupta S, Ahmad N, Agarwal MK, Agarwal ML and Mukhtar H. Role of p53 and NF-kappaB in epigallocatechin-3-gallate-induced apoptosis of LNCaP cells. Oncogene 2003; 22: 4851-4859.
[57] Chow HH, Hakim IA, Vining DR, Crowell JA, Ranger-Moore J, Chew WM, Celaya CA, Rodney SR, Hara Y and Alberts DS. Effects of dosing condition on the oral bioavailability of green tea catechins after single-dose administration of polyphenon E in healthy individuals. Clin Cancer Res 2005; 11: 4627-4633.
[58] Komori A, Yatsunami J, Okabe S, Abe S, Hara K, Suganuma M, Kim SJ and Fujiki H. Anticarcinogenic activity of green tea polyphenols. Jpn J Clin Oncol 1993; 23: 186-190.
[59] Sarma DN, Barrett ML, Chavez ML, Gardiner P, Ko R, Mahady GB, Marles RJ, Pellicore LS, Giancaspro GI and Low Dog T. Safety of green tea extracts: a systematic review by the US pharmacopeia. Drug Saf 2008; 31: 469-484.
[60] Mazzanti G, Di Sotto A and Vitalone A. Hepatotoxicity of green tea: an update. Arch Toxicol 2015; 89: 1175-1191.
[61] Shanafelt TD, Call TG, Zent CS, Leis JF, LaPlant B, Bowen DA, Roos M, Laumann K, Ghosh AK, Lesnick C, Lee MJ, Yang CS, Jelinek DF, Erlichman C and Kay NE. Phase 2 trial of daily, oral polyphenon E in patients with asymptomatic, Rai stage 0 to II chronic lymphocytic leukemia. Cancer 2013; 119: 363-370.

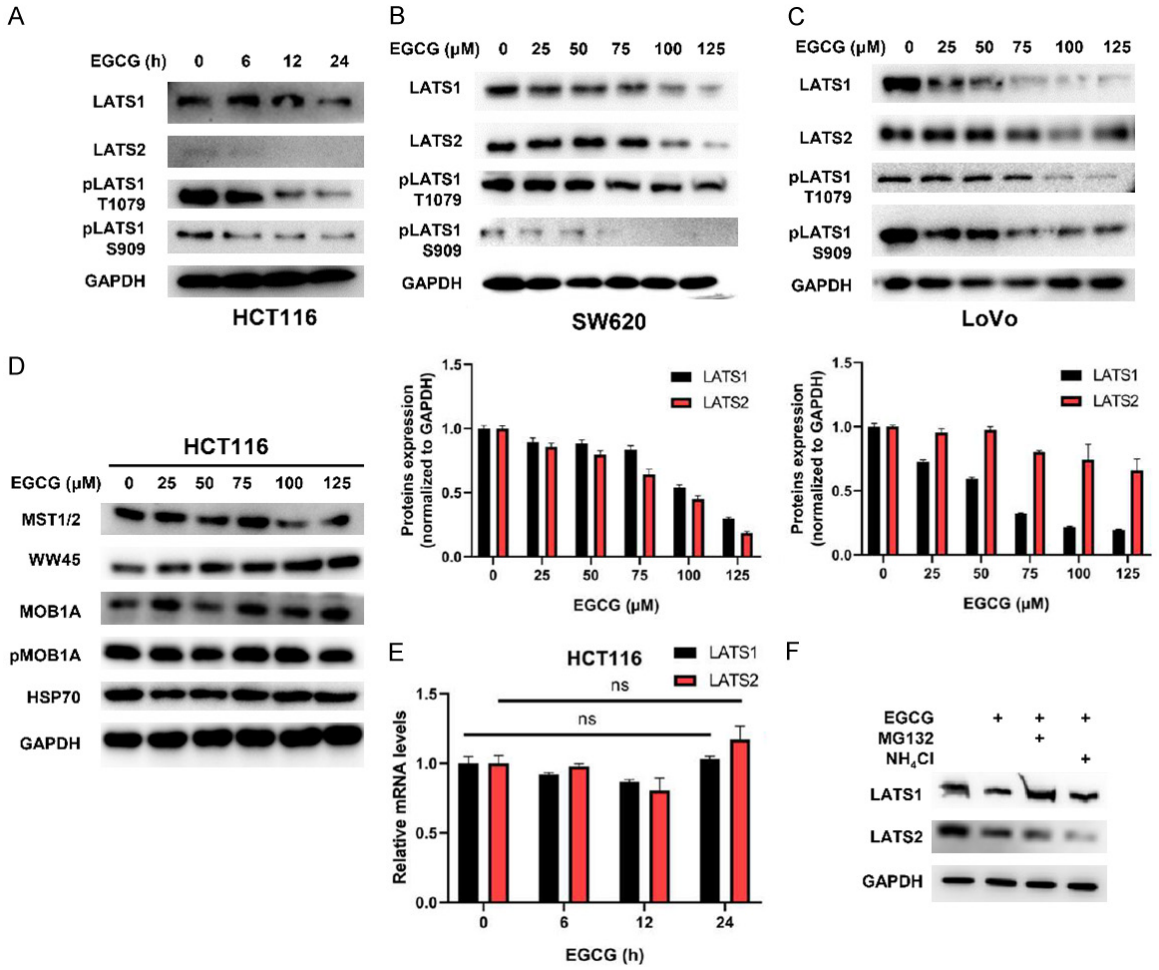

Figure S1. EGCG regulates the degradation of LATS1/2 protein, not mRNA degradation or upstream regulation. (A) Subconfluent HCT116 cells were treated with 100 μM of EGCG for the indicated times. After treatment, cell lysates were analyzed by immunoblotting for the indicated antigens. (B and C) SW620 cells (B) and LoVo cells (C) were treated with EGCG at concentrations of 0, 25, 50, 75, 100 and 125 μM for 24 hr. After treatment, cell lysates were analyzed by immunoblotting for the indicated antigens. An example blot is shown on the upon, summary data on the bottom. Data were expressed as mean ± SD of three independent experiments. (D) Subconfluent HCT116 cells were treated with EGCG at concentrations of 0, 25, 50, 75, 100 and 125 μM for 24 hr. After treatment, cell lysates were analyzed by immunoblotting for the indicated antigens. (E) HCT116 cells were treated with EGCG as the same as in the (A), levels of LATS1 and LATS2 mRNA were assayed by qRT-PCR. (F) 24 hr after EGCG treatment, cells were treated with 50 μM MG132 or 50 μM NH_4Cl for 6 hr and lysates were subjected to western blotting analysis.

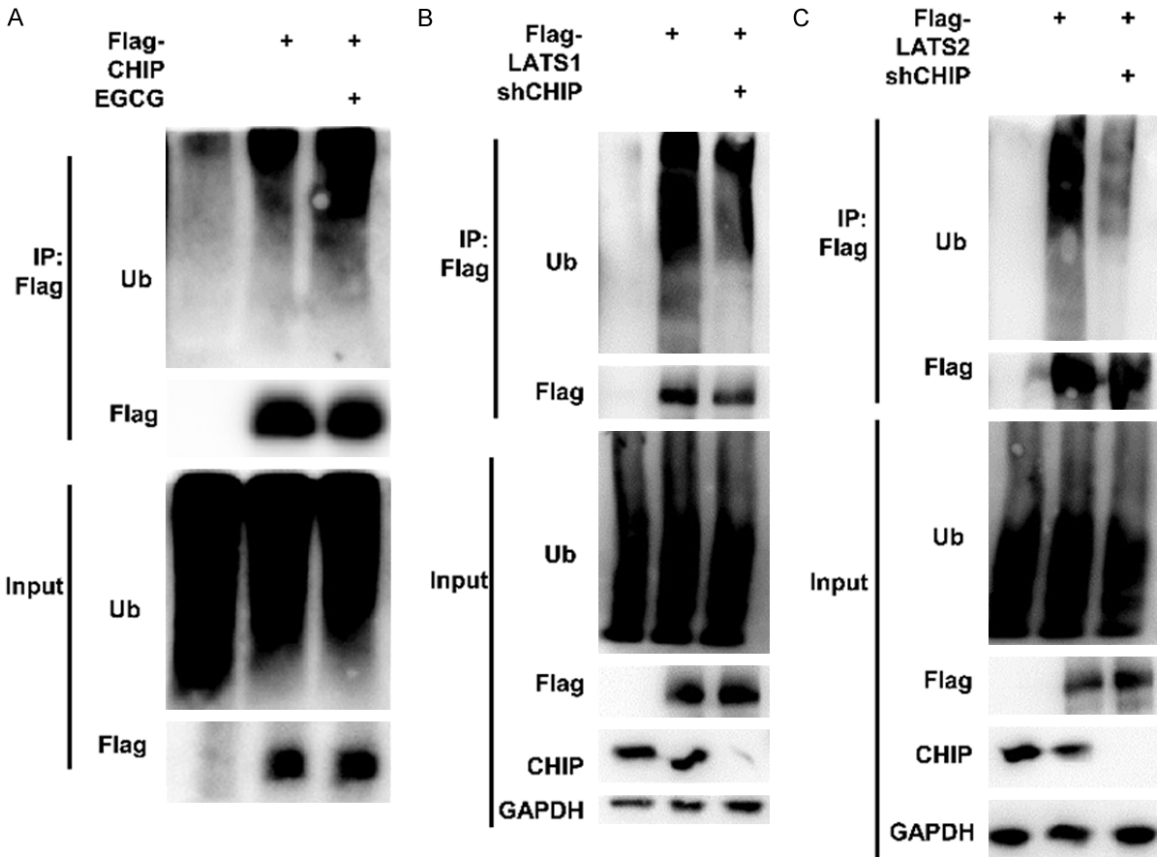

Figure S2. EGCG activates CHIP's E3 ubiquitin ligase activity and CHIP knockdown inhibits LATS1/2 poly-ubiquitination. (A) EGCG activates CHIP's E3 ubiquitin ligase activity. HCT116 cells were transfected with Flag-CHIP, 42 hours post-transfection, cells were treated with 100 μM EGCG and 20 μM MG132 for another 6 hr. Cell lysates were immunoprecipitated with anti-Flag antibody, followed by IB with indicated antibodies. (B and C) CHIP knockdown inhibits LATS1/2 poly-ubiquitination. HCT116 cells were infected with either scrambled-shRNA or CHIP-shRNA lenti-viruses. 72 hr after infection, cells were transfected with Flag-LATS1 (B) or Flag-LATS2 (C), 42 hr post-transfection, cells were treated with 20 μM MG132 for another 6 hr. Cell lysates were immunoprecipitated with anti-Flag antibody, followed by IB with indicated antibodies.

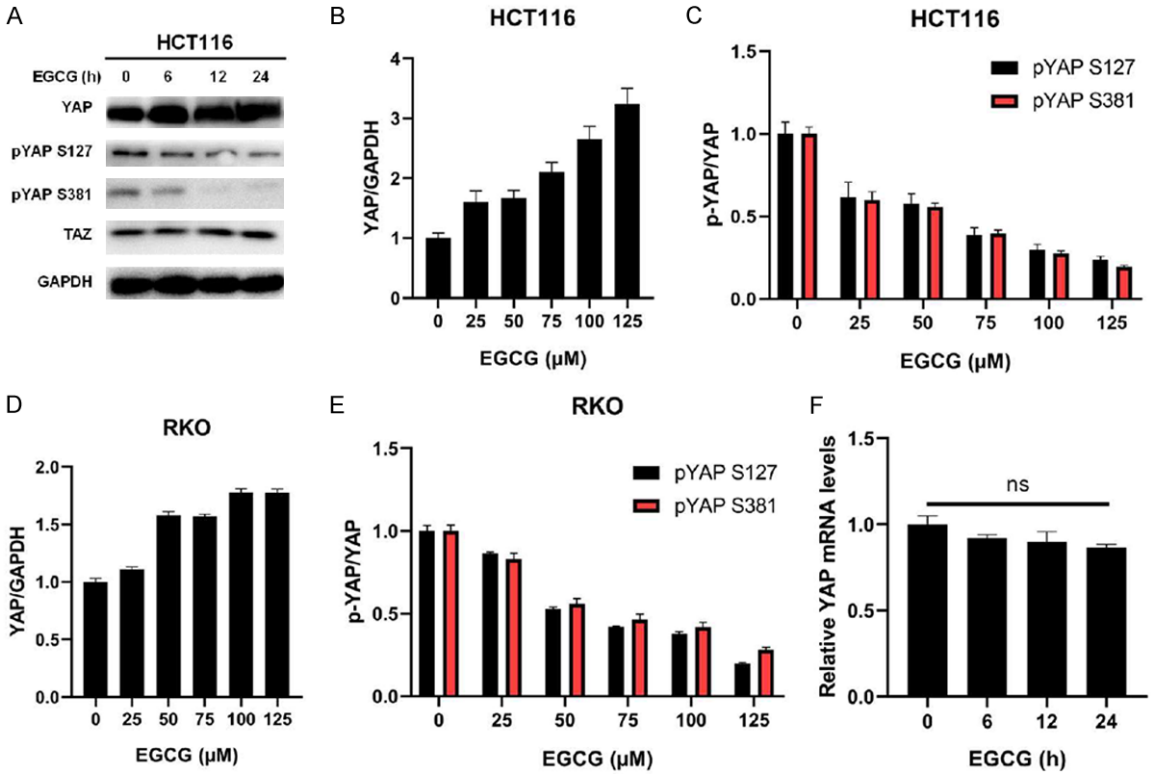

Figure S3. EGCG regulates YAP protein, not mRNA. (A) Subconfluent HCT116 cells were treated with 100 μM of EGCG for the indicated times. After treatment, cell lysates were analyzed by immunoblotting for the indicated antigens. (B and C) Summary analysis for immunoblots displayed in **Figure 3A**. Data were expressed as mean ± SD of three independent experiments. (D and E) Summary analysis for immunoblots displayed in **Figure 3B**. Data were expressed as mean ± SD of three independent experiments. (F) HCT116 cells were treated with EGCG as the same as in the (A), levels of YAP mRNA were assayed by qRT-PCR.

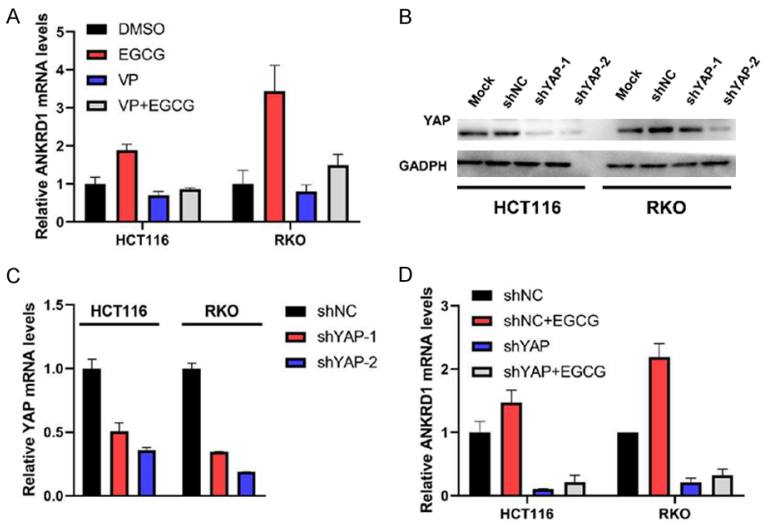

Figure S4. EGCG upregulates the mRNA expression of ANKRD1. (A) The mRNA expression level of ANKRD1 in RKO and HCT116 cell samples from **Figure 3F** was analyzed by qPCR. (B and C) Western Blot (B) and qPCR (C) were used to analyze the protein and mRNA expression levels of YAP in HCT116 and RKO cell lines with YAP knockdown. (D) The mRNA expression level of ANKRD1 in RKO and HCT116 cell samples from **Figure 3H** was analyzed by qPCR.